$$\mathrm{CdS} \xrightarrow{h\nu} \mathrm{e^-_{CB}} + \mathrm{h^+_{VB}} \qquad (10)$$

Although most of e^-_{CB} recombines with h^+_{VB}, some are trapped. Recombination of a small fraction of the charge species, generated either by bandgap irradiation (eq 10) or from those subsequently detrapped, results in fluorescence. MV^{2+} removes some electrons competitively:

$$\mathrm{MV^{2+}} + \mathrm{e^-_{CB}} \rightarrow \mathrm{MV^{\bullet +}} \qquad (11)$$

and thus decreases the fluorescence yield (Figure 6). The absorption spectra seen in Figure 7 corresponds to $MV^{\bullet +}$, the product of reaction 11. The function of benzyl alcohol is to remove h^+_{VB} and, thus, increase the yield of $MV^{\bullet +}$. Significantly, size quantization has not only manifested in bandgap shifts and in the appearance of exciton fluorescence but has also affected photoelectron transfer efficiencies.

In summary, ultrathin membranes prepared from carefully selected polymer blends provide, therefore, unique matrices for the in situ generation of uniform size-quantized semiconductor particles and for the examination of vectorial photoelectron transfer therein.

Acknowledgment. Support of this work by a grant from the National Science Foundation (to J.H.F.) is gratefully acknowledged. J.H.F. and I.C. are members of the Center for Membrane Engineering and Science at Syracuse University.

Registry No. CA, 9004-35-7; PSP, 34823-60-4; CdS, 1306-23-6; MV^{2+}, 1910-42-5.

NMR Chemical Shift Tensors and Peak Assignments for the 6H Polytype of Silicon Carbide

Mary Frances Richardson,* J. Stephen Hartman,* Deqi Guo, and
Beatrice G. Winsborrow

Department of Chemistry, Brock University, St. Catharines, Ontario L2S 3A1, Canada

Received July 29, 1991. Revised Manuscript Received December 3, 1991

^{29}Si and ^{13}C chemical shift tensors have been determined for single crystals of 6H SiC and are assigned to each of the crystallographically distinct sites (three silicon and three carbon) on the basis of symmetry arguments. The tensor components are dramatically dependent upon the number and geometrical arrangement of second neighbors but are not appreciably affected by the very slight variations in bond distances among the different sites.

Our magic angle spinning (MAS) NMR studies of silicon carbide polytypes[1,2] showed that the different polytypes, and crystallographically distinct silicons (and carbons) within the same polytype, give distinctive isotropic chemical shifts. The range of chemical shifts in the 6H polytype is roughly 10 ppm for ^{29}Si and 8 ppm for ^{13}C. These chemical shift differences among lattice sites seem remarkably large, considering that the chemical environments appear to be practically identical, the range of bond distances in the Si–C tetrahedra is less than 0.01 Å, and the bond angles are all 109.4–109.5°.[3] The simplicity of the silicon carbide structure combined with the range of NMR chemical shifts make silicon carbide an excellent compound for exploring the general problem of chemical shifts in network solids.

Silicon carbide polytypes have layer-type structures in which the layers are identical but the stacking sequences of the layers differ.[4-7] Thus, although the first-neighbor surroundings of each Si (or C) are quite similar, the second-neighbor surroundings can be different, depending on the stacking sequences of the layers. We[1,2] and others[8,9] proposed that the number of NMR peaks is related to the ways that layers can be stacked about a central atom. There are only four independent stacking sequences within a 5-Å radius, denoted as types A–D. Figure 1 shows diagrams of the four types, with an SiC_4 tetrahedron embedded in the second-neighbor polyhedron. Of the crystallographically independent silicons in 6H SiC, one is type A, one is type B, and one is type C, corresponding to the three equal-intensity peaks in the ^{29}Si MAS NMR spectrum. The carbon atoms in any polytype are isostructural to the silicon atoms, so the ^{13}C spectrum of the 6H polytype also has three equal-intensity peaks corresponding to type A, type B, and type C carbons. O'Keeffe's topological approach to site classification gives similar results.[9]

However, unambiguous assignment of NMR peaks to specific sites in the crystal lattice has proved elusive.[2,8,10] Additional interactions beyond the 5-Å radius must have appreciable effects on chemical shift, since the 15R polytype, which has five crystallographically distinct carbon sites but with only types A–C represented, has four rather than three ^{13}C peaks.[2] Also the recently reported[10] ^{29}Si and ^{13}C chemical shifts of the 4H polytype (with only types B and C represented) are distinctly different from chemical

---

[1] Finlay, G. R.; Hartman, J. S.; Richardson, M. F.; Williams, B. L. *J. Chem. Soc., Chem. Commun.* **1985**, 159–161.

[2] Hartman, J. S.; Richardson, M. F.; Sherriff, B. L.; Winsborrow, B. G. *J. Am. Chem. Soc.* **1987**, *109*, 6059–6067.

[3] Gomes de Mesquita, A. H. *Acta Crystallogr.* **1967**, *23*, 610–617.

[4] Verma, A. R.; Krishna, P. *Polymorphism and Polytypism in Crystals*; John Wiley and Sons: New York, 1966.

[5] Schaffer, P. T. B. *Acta Crystallogr.* **1969**, *B25*, 477–488.

[6] Pandey, D.; Krishna, P. Polytypism in Close-Packed Structures. In *Current Topics in Materials Science*; Kaldis, E., Ed.; North-Holland Publishing Company: Amsterdam/New York, 1982.

[7] *Gmelin Handbook of Inorganic Chemistry*, 8th ed.; Schlichting, J., Czack, G., Koch-Bienemann, E., Kuhn, P., Schroder, F., volume authors; Springer-Verlag: Berlin, 1984; Suppl. *Vol.* B2, Si-Silicon, "Properties of Crystalline Silicon Carbide".

[8] Guth, J. R.; Petuskey, W. T. *J. Phys. Chem.* **1987**, *91*, 5361–5364.

[9] O'Keeffe, M. *Chem. Mater.* **1991**, *3*, 332–335.

[10] Apperley, D. C.; Harris, R. K.; Marshall, G. L.; Thompson, D. P. *J. Am. Ceram. Soc.* **1991**, *74*, 777–782.

0897-4756/92/2804-0318$03.00/0

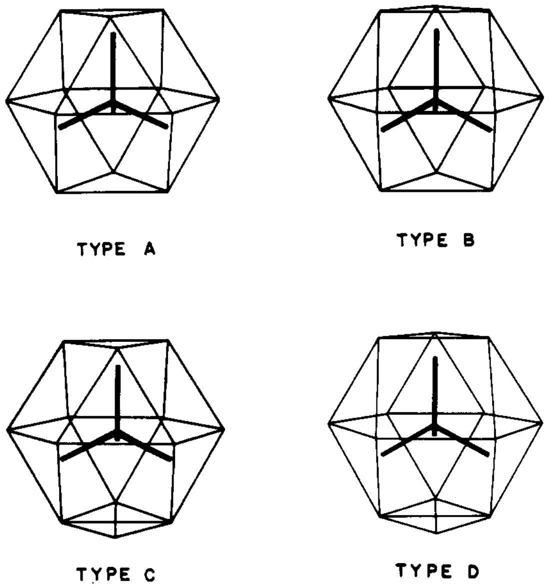

Figure 1. The four types of surroundings in silicon carbide polytypes, out to the second-neighbor shell.

shifts of other polytypes which also have types B and C sites. O'Keeffe[9] showed that there are 6 topologically distinct sites out to a distance of 7.6 Å, and we showed that there are 16 geometrically distinct sites out to this distance;[2] the topological and geometrical classifications differ in that some geometrically different polyhedra are topologically equivalent.

Chemical shift tensors contain much more information than the isotropic shifts which are obtained from MAS NMR spectra. The three principal tensor components can vary individually as structure varies,[11] and the isotropic shift is an average of these. It is the tensor components that can reveal most dramatically the effects of changes in local structure and symmetry on the chemical shift. Thus nuclear shielding can change significantly with bond distance, sometimes by more than 1000 ppm/Å.[12,13] Such changes may strongly affect only one of the tensor components and can be obscured if only the isotropic shift is considered. Good correlations have been found between single-crystal shift tensor components and bond distances in silicates and other systems.[11,13-17]

Silicon carbide is an important industrial material and is one of the most promising materials in the rapidly developing field of high-temperature ceramics.[18] High-resolution solid-state NMR spectroscopy has great potential in studying such materials.[19] In the past few years, NMR has become an important technique for monitoring the formation of silicon carbide from polymer precursors[20] and from other sources.[21] The present work is aimed at developing further insight into chemical shift–structure relationships in silicon carbide.

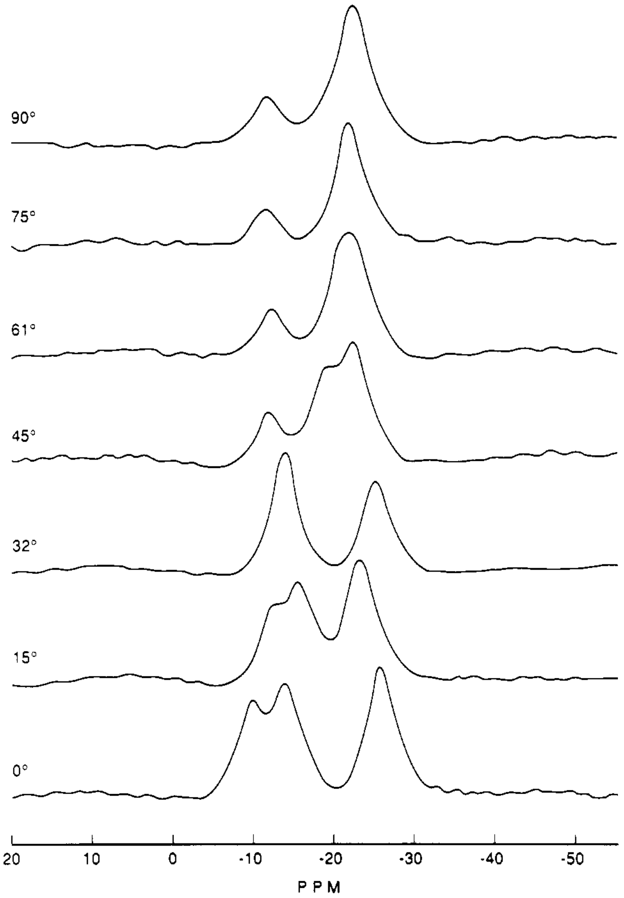

Figure 2. Single-crystal ^{29}Si NMR spectrum of 6H SiC (crystal A) as a function of angle between the magnetic field and the c axis of the crystal.

Experimental Section

NMR studies were performed on production-run silicon carbide crystals supplied by the General Abrasive division of Dresser Industries, Niagara Falls, Ontario. Precession photographs confirmed that the crystals were 6H SiC. The absence of streaking and extra spots indicated that there was negligible disorder and no other polytype present in significant amounts.

Single-crystal ^{29}Si and ^{13}C spectra were obtained at 39.7 and 50.3 MHz, respectively, on a Bruker AC-200 multinuclear Fourier transform NMR spectrometer using a standard Bruker high-resolution probe (nonspinning). Series of spectra were acquired at different orientations of the crystal c axis with respect to the external magnetic field by mounting the crystal on angled glass wedges inserted into a 10-mm NMR tube. Since the crystals have hexagonal symmetry, there was no need to orient a and b axes in specific directions. Most of the best single crystals were thin,

---

(11) Facelli, J. C.; Grant, D. M.; Michl, J. *Acc. Chem. Res.* **1987**, *20*, 152–158.

(12) Chesnut, D. B. *Annu. Rep. NMR Spectrosc.* **1989**, *21*, 51–97.

(13) Grimmer, A. R. *Chem. Phys. Lett.* **1985**, *119*, 416–420.

(14) Spearing, D. R.; Stebbins, J. F. *Am. Mineral.* **1989**, *74*, 956–959.

(15) Griffith, E. A. H.; Li, H. Y.; Amma, E. L. *Inorg. Chim. Acta* **1988**, *148*, 203–208.

(16) Un, S.; Klein, M. P. *J. Am. Chem. Soc.* **1989**, *109*, 5119–5124.

(17) Harris, R. K.; Pritchard, T. N.; Smith, E. G. *J. Chem. Soc., Faraday Trans. 1* **1989**, *85*, 1853–1860.

(18) Aldinger, F.; Kalz, H.-J. *Angew. Chem., Int. Ed. Engl.* **1987**, *26*, 371–381. Ulrich, D. R. *Chem. Eng. News* **1990**, *68* (Jan 1), 28–40.

(19) Hatfield, G. R.; Carduner, K. R. *J. Mater. Sci.* **1989**, *24*, 4209–4219. Turner, G. L.; Kirkpatrick, R. J.; Rusbud, S. H.; Oldfield, E. *Am. Ceram. Soc. Bull.* **1987**, *66*, 656–663. Dupree, R.; Holland, D. In *Glasses and Glass-Ceramics*; Lewis, M. H., Ed.; Chapman and Hall; London, 1989; pp 1–40. Eckert, H. *Ber. Bunsenges. Phys. Chem.* **1990**, *94*, 1062–1085.

(20) Zhang, Z.-F.; Babonneau, F.; Laine, R. M.; Mu, Y.; Harrod, J. F.; Rahn, J. A. *J. Am. Ceram. Soc.* **1991**, *74*, 670–673. Schmidt, W. R.; Interrante, L. V.; Doremus, R. H.; Trout, T. K.; Marchetti, P. S.; Maciel, G. E. *Chem. Mater.* **1991**, *3*, 257–267. Lipowitz, J.; Freeman, H. A.; Chen, R. T.; Prack, E. R. *Adv. Ceram. Mater.* **1987**, *2*, 121–128. Taki, T.; Inui, M.; Okamura, K.; Sato, M. *J. Mater. Sci. Lett.* **1989**, *8*, 918–920. Murthy, V. S. R.; Lewis, M. H.; Smith, M. E.; Dupree, R. *Mater. Lett.* **1989**, *8*, 263–268.

(21) Carduner, K. R.; Shinozaki, S. S.; Rokosz, M. J.; Peters, C. R.; Whalen, T. J. *J. Am. Ceram. Soc.* **1990**, *73*, 2281–2286. Dando, N. R.; Tadayyoni, M. A. *J. Am. Ceram. Soc.* **1990**, *73*, 2242–2246. Inkrott, K. E.; Wharry, S. M.; O'Donnell, D. J. *Mater. Res. Soc. Symp. Proc.* **1986**, *73*, 165–171. Wagner, G. W.; Na, B.-K.; Vannice, M. A. *J. Phys. Chem.* **1989**, 93, 5061–5064. Julbe, A.; Larbot, A.; Guizard, C.; Cot, L.; Dupin, T.; Charpin, J.; Bergez, P. *Eur. J. Solid State Inorg. Chem.* **1989**, *26*, 101–111. Marshall, G. L.; Harris, R. K.; Apperley, D.; Yeung, R. *Proc. Symp. Sci. Ceram.* **1988**, *14*, 347–352.

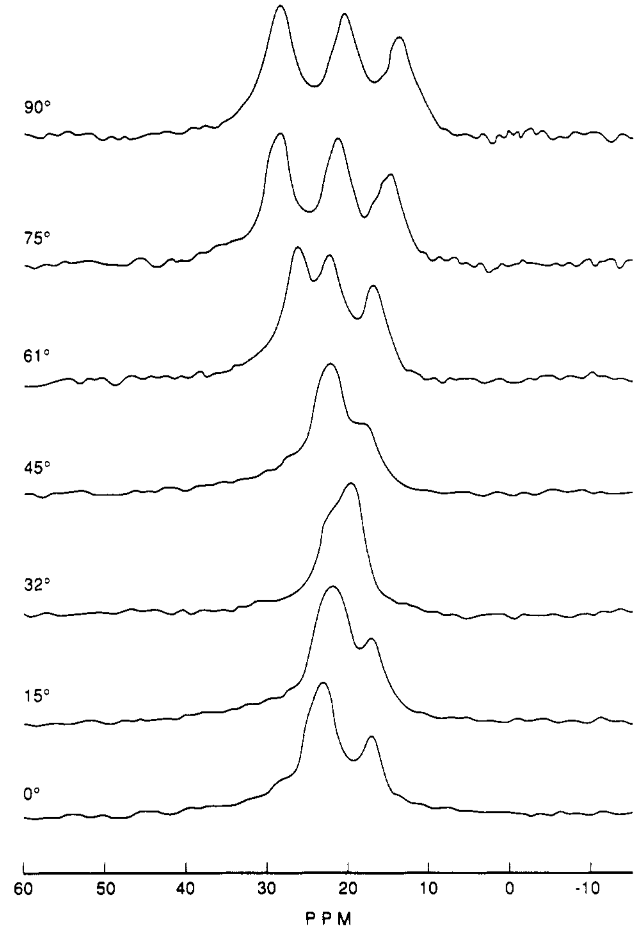

Figure 3. Single-crystal ^{13}C NMR spectrum of 6H SiC (crystal A) as a function of the angle between the magnetic field and the *c* axis of the crystal.

Table I. ^{29}Si and ^{13}C Chemical Shift Tensors for 6H SiC

curve	δ_{11}	δ_{33}	$\delta_{33} - \delta_{11}$	$\bar{\delta}$	δ_{MAS}[2]	assgt
			Crystal A			
silicon						
a	−11.6	−14.9	−3.3	−12.7	−14.5	Si(3)
b	−21.7	−26.5	−4.8	−23.3	−25.1	Si(1)
c	−22.7	−10.7	12.0	−18.7	−20.6	Si(2)
carbon						
a	21.5	22.9	1.4	22.0	20.4	C(2)
b	14.7	22.0	7.3	17.1	15.1	C(1)
c	29.3	16.3	−13.0	24.6	23.7	C(3)
			Crystal B			
silicon						
a	−12.5	−11.5	1.0	−12.2	−14.5	Si(3)
b	−23.5	−23.0	0.5	−23.2	−25.1	Si(1)
c	−23.6	−7.6	16.0	−18.3	−20.6	Si(2)
carbon						
a	20.1	25.6	5.5	21.9	20.4	C(2)
b	13.0	25.6	12.5	17.2	15.1	C(1)
c	28.0	20.1	−7.9	25.4	23.4	C(3)

[a] Reference 2.

and attempts were made to increase the thickness, and hence the signal intensity, by stacking several thin crystals. However the resolution was poor in the resulting spectra. Spectral resolution varied considerably among a number of large blue-black crystals. The two thick single crystals that gave the sharpest NMR peaks are referred to as crystal A (5 × 5 × 5 mm) and crystal B (10 × 5 × 3 mm). The ^{29}Si and ^{13}C NMR spectra obtained with crystal A are shown in Figures 2 and 3, respectively. ^{29}Si and ^{13}C chemical shifts were referenced to external tetramethylsilane and are reported in ppm to low field of tetramethylsilane.

^{29}Si spectra were obtained as a sum of 1800 scans with a relaxation delay of 30 s between scans. ^{13}C spectra were obtained as a sum of 2700 scans with a relaxation delay of 20 s between scans. For both nuclei 15° pulses, 8K data points, and 16 000 Hz spectral windows were used, and the spectra were Fourier transformed with 25 Hz of line broadening applied. Spectra consisting of overlapping peaks were simulated using LINESIM, a simplex iterative fitting program written by Dr. Peter Barron and available as part of the Bruker program library (ABACUS, Catalog no. ABA051).

Results and Discussion

Single-Crystal Spectra and Comparison to MAS NMR Spectra. Plots of chemical shift versus orientation angle are shown in Figures 4–7 for crystals A and B. Because of the high crystal symmetry, the shift tensor must have one of its principal components (δ_{33}) aligned along the crystal *c* axis (6-fold axis) and be cylindrically symmetrical ($\delta_{11} = \delta_{22}$).[22] Thus there are only two components to be determined for each atom: δ_{11} and δ_{33}, the shifts in the *x* and *z* directions. These quantities were determined from a least-squares fit to eq 1, which relates the observed

$$\delta = \delta_{11} \sin^2 \theta + \delta_{33} \cos^2 \theta \qquad (1)$$

shift of a given atom to θ, the angle between the *c* axis and the magnetic field. Values of δ_{11} and δ_{33} for each atom are given in Table I, along with the chemical shift anisotropy ($\delta_{33} - \delta_{11}$).

The two crystals do not give identical spectra and shift tensor components, although they do give average chemical shifts (isotropic shifts) that are the same within experimental error (Table I). Mounting crystals on "slopes" in a standard high-resolution NMR tube, due to unavailability of a goniometer-head NMR probe, is unlikely to have introduced errors greater than 2–3° in orientation angle. The discrepancies between the two crystals are apparently related to varying impurity levels and defects; industrial silicon carbide samples normally contain impurities,[4] and nonstoichiometry is common.[7,23]

That real sites need not approach too closely to the ideal symmetry of the crystal is supported by our observation that magic angle spinning sharpens the ^{29}Si signal in cubic (3C) silicon carbide, whereas the cubic symmetry of the crystal implies that MAS should have no effect. The same result was found in a ^{13}C NMR study of diamond: gem-quality diamond gave a sharp signal in the absence of MAS, but industrial diamond powders of the same nominal cubic symmetry required MAS.[24] Local defects and impurities must lower the local symmetry, thus affecting the individual shift tensors and broadening the observed peaks, which are superpositions of the signals arising from all of the atoms in given sites.

Also shown in Table I is the average value of the principal components, $\bar{\delta} = {}^1/_3(2\delta_{11} + \delta_{33})$, which should be equivalent to the isotropic shift observed in MAS NMR.[2] There is a discrepancy averaging about 1.7 ppm, with the MAS value always to high field of the average value of the principal components. This is a crystal vs powder effect, since grinding of crystal B led to ^{13}C and ^{29}Si MAS NMR chemical shifts of the powder which are typical of 6H SiC, i.e., 1.5–2 ppm to high field of the average of the single-

---

(22) Weil, J. A.; Buch, T.; Clapp, J. E. *Adv. Magn. Reson.* **1973**, *6*, 183–257.

(23) *Gmelin Handbook of Inorganic Chemistry*, 8th ed.; Haase, V., Kirschstein, G., List, H., Ruprecht, S., Sangster, R., Schroder, F., Topper, W., Vanecek, H., Heit, W., Schlichting, J., volume authors; Springer-Verlag: Berlin, 1986; Suppl. *Vol.* B3, Si-Silicon, "System Si–C".

(24) Henrichs, P. M.; Cofield, M. L.; Young, R. H.; Hewitt, J. M. *J. Magn. Reson.* **1984**, *58*, 85–94.

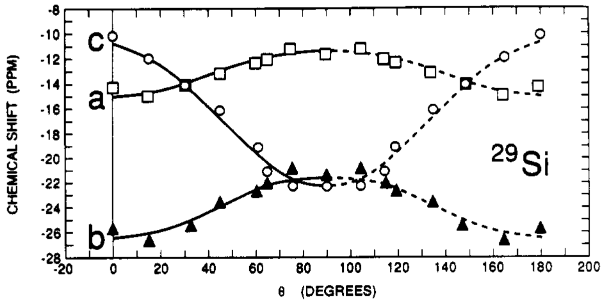

Figure 4. Angular dependence of the ^{29}Si NMR lines for crystal A of 6H SiC.

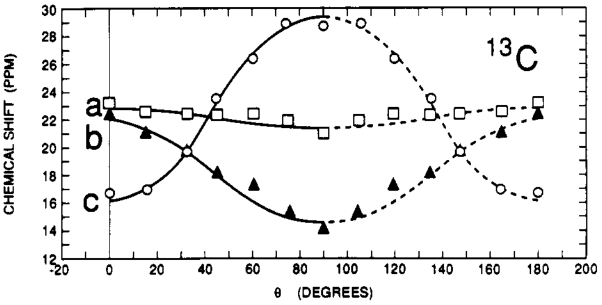

Figure 5. Angular dependence of the ^{13}C NMR lines for crystal A of 6H SiC.

crystal principal components. Differences of comparable magnitude between the MAS NMR isotropic shift and the average value of the shift tensor are present in other systems, e.g., Mg_2SiO_4.[25,26] Effects of this magnitude are small compared to the usual range of ^{29}Si chemical shift anisotropies in typical silicates (e.g., ref 25) but are proportionately much larger and therefore more noticeable in the highly symmetric silicon carbide sites with their small chemical shift anisotropies.

Differences between the MAS NMR shifts and the average values of the shift tensors are thought to arise from anisotropy in the bulk magnetic susceptibility of the sample.[27] Hexagonal silicon carbide does indeed have an anisotropic magnetic susceptibility, which varies considerably among samples and is attributable to variations in the nature and amount of impurities and defects in the crystals.[28]

Peak Assignments in the Single-Crystal Spectra. The shapes of the ^{13}C curves approximately mirror the shapes of the ^{29}Si curves for crystal A (Figures 4 and 5), although the relative chemical shift positions of the two sets of curves are different for the two nuclei. This mirroring disappears for the curves obtained for crystal B, in which two ^{29}Si sites show negligible dependence of chemical shift on orientation (Figures 6 and 7). In both sets of ^{13}C and ^{29}Si spectra, there is one curve that has an opposite orientation angle dependence from the other two. In the ^{29}Si spectra (Figures 4 and 6), one of the silicons is much more strongly deshielded when the *c* axis is parallel to the magnetic field than when it is perpendicular, whereas the other two silicons are somewhat more deshielded when the *c* axis is perpendicular to the magnetic field (crystal A) or the shielding is essentially constant (crystal B). In the ^{13}C spectra (Figures 5 and 7), one of the carbons is very strongly shielded when the *c* axis is parallel to the magnetic field. The other two carbons exhibit higher shielding when the *c* axis is perpendicular to the magnetic field.

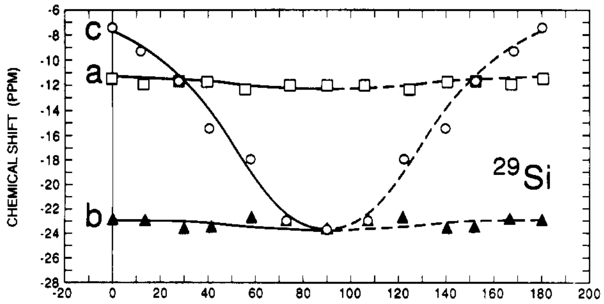

Figure 6. Angular dependence of the ^{29}Si NMR lines for crystal B of 6H SiC.

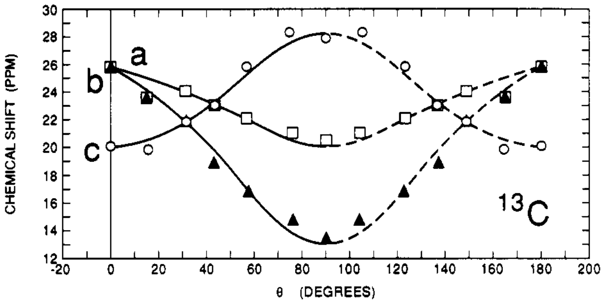

Figure 7. Angular dependence of the ^{13}C NMR lines for crystal B of 6H SiC.

Several authors[12-14] have correlated principal values of the chemical shift tensor with the bond distances in the direction of the tensor eigenvectors. This approach fails with 6H SiC even though the vertical bonds are as much as 0.008 ± 0.002 Å longer than the lateral bonds.[3] If the chemical shift variation with distance were a significant factor for explaining the curve shapes in Figures 4–7, all curves for Si (or C) would vary in the same sense with orientation angle. The possibility that lateral bonds for some of the atoms might be longer than the vertical bonds is remote, given the accuracy of the 6H structure[3] and the elongation of the *c* axis in all known hexagonal polytypes.[8] Further, the curves for Si should have the same anisotropy direction as the curves for C, since $d\sigma/dr$ [$=-d\delta/dr$] is almost always negative for *both* atoms in the bond being stretched.[12] We thus conclude that the chemical shift differences observed for 6H SiC are not due to variations in bond distances to nearest neighbors.

The mirror symmetry in the shapes of the ^{13}C and ^{29}Si curves for crystal A strongly suggests a link between structurally alike silicons and carbons and on this basis we consider the symmetry of the second-neighbor surroundings. Two of the independent silicons have 12 second-nearest neighbors (all silicons), but the third has 13 (12 Si + 1 C), with the carbon located on the *z* axis (Figure 1). Similarly, two of the carbons have 12 carbons as second-nearest neighbors, but the third has 13 second-nearest neighbors (12 C + 1 Si). The thirteenth atom, at a distance of just over 3.1 Å, should have a pronounced effect on the *z* component of the tensor. We thus assign curves c in Figures 4 and 5 to the type C atoms in 6H SiC, i.e., to Si(2) and C(3). (The silicon and carbon numbers correspond to the crystallographic labels.[3])

Curves a in Figures 4 and 5 exhibit the least anisotropy, and this points to the most symmetrical environment. A perfect crystal of cubic 3C SiC would show no anisotropy at all because of the high symmetry. We thus assign these

---

[25] Weiden, N.; Rager, H. *Z. Naturforsch.* **1985**, *40A*, 126–130.

[26] Magi, M.; Lippmaa, E.; Samoson, A.; Engelhardt, G.; Grimmer, A. R. *J. Phys. Chem.* **1984**, *88*, 1514. Smith, K. A.; Kirkpatrick, J.; Oldfield, E.; Henderson, D. M. *Am. Mineral.* **1983**, *68*, 1206.

[27] Earl, W. L.; VanderHart, D. L. *J. Magn. Reson.* **1982**, *48*, 35–54.

[28] Das, D. *Indian J. Phys.* **1967**, *41*, 525–532. Reference 7, pp 170–171.

Table II. Chemical Shift Assignments for 6H SiC

chem shift	ref 2	ref 8	ref 10	this work
		Silicon		
−14.5	Si(3)	Si(3)	Si(3)	Si(3)
−20.4	Si(1) or Si(2)	Si(2)	Si(1)	Si(2)
−25.1	Si(2) or Si(1)	Si(1)	Si(2)	Si(1)
		Carbon		
15.1	C(2)		C(1)	C(1)
20.4	C(1) or C(3)		C(3)	C(2)
23.4	C(3) or C(1)		C(2)	C(3)

curves to Si(3) and to C(2), respectively, as the cubic type A surroundings are inherently more symmetrical than the hexagonal type B sites. This leaves curves b in Figures 5 and 6. Their moderate anisotropy is consistent with assigning them to Si(1) and C(1), in type B sites.

We noted previously[1,2] that the isotropic ^{29}Si and ^{13}C MAS NMR chemical shifts of 6H SiC seemed to mirror each other, i.e., the positions and relative separations of the ^{29}Si peaks at −14.5, −20.4, and −25.1 ppm were reflected in the ^{13}C peaks at 15.1, 20.4, and 23.4 ppm. This mirroring in the isotropic shifts is fortuitous, as it does not correspond to the mirroring in the angular dependence of the single-crystal spectra. Curve c in Figure 4 is the mirror (in shape) of curve c in Figure 5, but the isotropic shifts represented by these two tensors are −20.4 and +23.4 ppm, i.e., the central peak in the ^{29}Si spectrum, but the lowest-field peak in the ^{13}C spectrum.

Table II summarizes our assignments for 6H SiC. Our ^{29}Si assignments are consistent with those of Guth and Petuskey[8] as well as with our previous work.[2] Our ^{13}C assignments differ from our previous ones,[2] as well as from those of Apperley et al., who assigned the A site by comparing peak positions in 6H SiC with those in 4H SiC which contains only B and C sites.[10] Previous assignments have rested on the assumption that a specific site type should be associated with a particular chemical shift even when the polytypes are different. This assumption is appealing (and we have used it ourselves[2]), but there is mounting evidence against it. Chemical shifts for a given site type can vary by several ppm in different polytypes,[10] and even for crystallographically different carbons of the same site type in the same polytype, as in 15R SiC.[2]

If peak separation is considered rather than peak position, then the 7.4 ppm separation of the two ^{13}C peaks corresponding to the B and C sites in 4H SiC[10] is not appreciably different from the 7.8 ppm separation of the highest- and lowest-field ^{13}C peaks in 6H SiC which we assign to the B and C sites.[2]

Electronic Structure, Chemical Shifts, and Anisotropy in the Shift Tensor. Variations in the shift tensor components for different sites in SiC polytypes may ultimately by explained by paramagnetic contributions which arise from nonspherical electron density distribution about an atom and are calculated from orbital overlaps between a central atom and its successive neighbors.[29] Their importance is clear in other systems: e.g., in $RbCaF_3$, the ^{19}F chemical shift anisotropy of 129 ppm is due almost entirely to F^- orbital overlaps with its first and second neighbors; contributions by the other atoms (out to 22 Å) accounted for only 6 ppm of the anisotropy.[30] The type C atoms in SiC are especially interesting in this regard, as a type C silicon has a type C carbon neighbor 3.1 Å away on the *z* axis. Electron density shifts from the silicon toward this carbon are consistent with the tensor assignments, in which the ^{29}Si curve showing strong deshielding in the *z* direction was assigned to type C silicon and the ^{13}C curve showing strong shielding in the *z* direction was assigned to type C carbon.

Others[31-33] have also shown that second and other near neighbors are important. Effects due to distant neighbors have been considered to be negligible since orbital overlaps and bond polarizations drop off rapidly with distance.[31]

Energy calculations indicate that the interactions to the first two layers are most important in determining polytype energies, and that interaction with the third layer is what stabilizes the 6H polytype over others.[34] These results are consistent with the idea that the main contributions to the chemical shift come from atoms within a few angstroms from the central atom, as we and others have suggested previously.[1,2,8,10,35]

We have also attempted to correlate chemical shifts in silicon carbide polytypes with long-range diamagnetic shielding due to point dipoles located on the Si–C bonds.[36] However, unreasonably large values of the bond susceptibility anisotropy must be used in order to obtain good agreement with the observed shifts, and this is consistent with the expected[29] predominance of paramagnetic over dimagnetic shielding terms.

Conclusions

Powerful two-dimensional NMR approaches based on connectivities are being developed for ^{29}Si NMR peak assignments in complex silicate structures,[37] but these are not always applicable: in 6H silicon carbide every silicon is connected (through carbon) to every type of silicon, so peaks cannot be assigned based on connectivity differences. The chemical shift tensor provides an alternative approach to assigning NMR signals, by making use of differences in site symmetry.

Hence more attention should be paid to the shift tensor rather than just to the isotropic shift, in order to get the most information from solid-state NMR. Shift tensor information for polycrystalline samples is becoming more readily available by high-resolution solid-state NMR experiments in which detection occurs under magic angle spinning conditions, but other portions of the experiment are carried out with the sample under other conditions: either static (stop-and-go spinning)[38] or with the spinner axis direction changed (switching-angle sample spinning, or spin flipping).[39] With a commercial probe now available

---

(29) Harris, R. K. *Nuclear Magnetic Resonance Spectroscopy*, revised edition; Longman Scientific and Technical: Essex, 1986; p 200.

(30) Kaliaperumal, R.; Sears, R. E. J.; Finch, C. B. *J. Chem. Phys.* **1987**, *87*, 68–72.

(31) (a) Sternberg, U. *Mol. Phys.* **1988**, *63*, 249–267. (b) Giessner-Prettre, C.; Pullman, A. *Chem. Phys. Lett.* **1985**, *114*, 258–260.

(32) Tenhover, M.; Boyer, R. D.; Henderson, R. S.; Hammond, T. E.; Shreve, G. A. *Solid State Commun.* **1988**, *65*, 1517–1521. (b) Brinkmann, D.; Freudenreich, W. *Z. Kristallogr.* **1976**, *143*, 67–78.

(33) Hallas, E.; Sternberg, U. *Mol. Phys.* **1989**, *68*, 315–326.

(34) Cheng, C.; Needs, R. J.; Heine, V. *J. Phys. C: Solid State Phys.* **1988**, *21*, 1049–1063.

(35) Carduner, K. R.; Blackwell, C. S.; Hammond, W. B.; Reidinger, F.; Hatfield, G. R. *J. Am. Chem. Soc.* **1990**, *112*, 4676–4679.

(36) Richardson, M. F.; Hartman, J. S.; Guo, D. Paper presented at the 29th Experimental NMR Conference, Rochester, NY, Apr 1988. Guo, D., M. Sc. Thesis, Brock University, St. Catharines, Ontario, Canada, 1988. Guo, D.; Hartman, J. S.; Richardson, M. F. *Can. J. Chem.*, in press.

(37) Fyfe, C. A.; Grondey, H.; Feng, Y.; Kokotailo, G. T. *J. Am. Chem. Soc.*, 1990, 112, 8812–8820 and references therein. Fyfe, C. A.; Feng, Y.; Grondey, H.; Kokotailo, G. T.; Mar, A. *J. Phys. Chem.* **1991**, *95*, 3747–3751.

(38) Zeigler, R. C.; Wind, R. A.; Maciel, G. E. *J. Magn. Reson.* **1988**, *79*, 299–306.

(39) Bax, A.; Szeverenyi, N. M.; Maciel, G. E. *J. Magn. Reson.* **1983**, *55*, 494–497. Terao, T.; Fujui, T.; Onodera, T.; Saika, A. *Chem. Phys. Lett.* **1984**, *107*, 145–148. Ashida, J.; Nakai, T.; Terao, T. *Chem. Phys. Lett.* **1990**, *168*, 523–528. Nakai, T.; McDowell, C. A. *J. Magn. Reson.* **1991**, *93*, 618–623.

Chem. Mater. **1992,** *4,* 323-330

for the switching-angle sample spinning experiment, we plan to use this method to extend our work.

Acknowledgment. We thank Mr. T. R. B. Jones for technical assistance, Dr. L. Wolfe and co-workers of General Abrasive, Niagara Falls, for access to production-run silicon carbide samples, and the Natural Sciences and Engineering Research Council of Canada for financial support in the form of operating grants to M.F.R. and J.S.H.

Registry No. SiC, 409-21-2.

Adsorption and Decomposition of Organophosphorus Compounds on Nanoscale Metal Oxide Particles. In Situ GC-MS Studies of Pulsed Microreactions over Magnesium Oxide

Yong-Xi Li, Olga Koper, Maher Atteya, and Kenneth J. Klabunde*

Department of Chemistry, Kansas State University, Manhattan, Kansas 66506

Received August 9, 1991. Revised Manuscript Received November 20, 1991

Using an in situ pulse reactor GC-MS system, the thermal decomposition of organophosphorus compounds (as models of nerve agents) has been compared with their destructive adsorption on high surface area magnesium oxide. Dramatically lower temperatures are required when MgO is present. Volatile products evolved were formic acid, water, alcohols, and alkenes. At higher temperatures CO, CH_4, and water predominated. Phosphorus residues remained completely immobilized. Addition of water enhanced the facility of MgO to destroy these compounds, and in fact, water pulses were found to partially regenerate a spent MgO bed. Using ^{18}O labeling, some aspects of the reaction mechanisms were clarified and in particular showed that oxygen scrambling occurred. Surface OH and MgO groups transferred oxygen in the formation of formic acid, and surface mobility and reactivity of adsorbed groups was very high. The substantial capacity of high surface area MgO for destruction and immobilization of such toxic substances makes it attractive for air purification schemes as well as solid reagents for destruction and immobilization of bulk quantities of hazardous phosphorus compounds or organohalides.

Introduction

Nanoscale metal oxide particles are proving to be effective new materials for adsorption and decomposition of large amounts of toxic materials.[1,2] The unique properties of these "destructive adsorbents" are due to their ultrahigh surface areas and high surface concentrations of reactive defect sites.

Two applications for these new adsorbents come to mind: (1) for air purification; (2) as reagents for destruction and immobilization of bulk quantities of hazardous chemicals. Both applications interest us, but we wish to draw attention to application 2 especially for organophosphorus compounds (as models of toxic nerve gases) and aromatic chlorocarbons (as models of polychlorobiphenyls). Herein we report more detailed studies of organophosphorus compound decomposition, while work on chlorinated hydrocarbons will be reported later.

Earlier investigators were mainly concerned with catalytic decomposition of toxic phosphorus compounds. Especially Weller and co-workers efforts with Pt/Al_2O_3 catalysts for air purification should be noted.[3-5] More general surface chemistry appraoches have been discussed by Ekerdt and co-workers,[2] and concern for the dangers of organophosphorus compounds appear in the fields of soil fertility, eutrophication, corrosion control, the detergent industry, and others.[6-8]

In examining the literature dealing with the catalytic or stoichiometric decomposition of organophosphorus compounds, we have noted a wide variety of differing results. A brief review of this literature follows.

Weller's early heterogeneous catalytic decomposition of isopropyl methylphosphonofluoridate, known as GB (nerve agents have similar structures such as GB (Sarin), GD or VX)),[2] and the simulant dimethyl methylphosphonate (DMMP) were studied with Pt/Al_2O_3, pure Al_2O_3, and amberlyst cation exchange resin under oxidizing conditions.[3-5,9] Between 300 and 400 °C, GB yielded CO_2, HF, H_2O, and H_3PO_4 (occurring as a viscous condensate near the sampling valve, although some reacted with the Al_2O_3 to form $AlPO_4$). As catalyst activity declined, the dealkylation product propene became the major product. With DMMP and Pt/Al_2O_3/air the products were CH_3OH and CO_2 while with N_2 flow, CH_3OH.

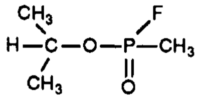

GB

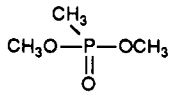

DMMP

Yates and co-workers have recently announced that a sustained heterogeneous catalytic decomposition of DMMP was achieved under oxidizing conditions on a

---

[1] (a) Li, Y. X.; Klabunde, K. J. *Langmuir* **1991,** *7,* 1388. (b) Li, Y. X.; Schlup, J. R.; Klabunde, K. J. *Langmuir* **1991,** *7,* 1394.

[2] Ekerdt, J. G.; Klabunde, K. J.; Shapley, J. R.; White, J. M.; Yates Jr., J. T. *J. Phys. Chem.* **1988,** *92,* 6182.

[3] Tzou, T.-Z.; Weller, S. W. Unpublished paper (private communication in 1991).

[4] Baier, R. W.; Weller, S. W. *Ind. Eng. Chem. Process Des. Dev.* **1967,** *6,* 380.

[5] Graven, W. M.; Weller, S. W.; Peters, D. L. *Ind. Eng. Chem. Process Des. Dev.* **1966,** *5,* 183.

[6] Parfitt, R. L.; Russell, J. D. *J. Soil Sci.* **1977,** *28,* 297.

[7] Lyklema, L. *Environ. Sci. Technol.* **1980,** *14,* 297.

[8] Strumm, W.; Furrer, G.; Kunz, B. *Croat. Chem. Acta* **1983,** 585.

[9] Graven, W. M.; Paton, J. D.; Weller, S. W. *Ind. Eng. Chem. Process Des. Dev.* **1966,** *5,* 34.

0897-4756/92/2804-0323$03.00/0